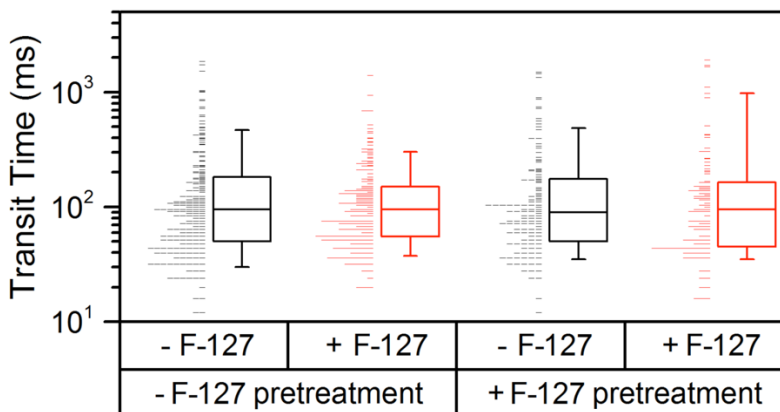
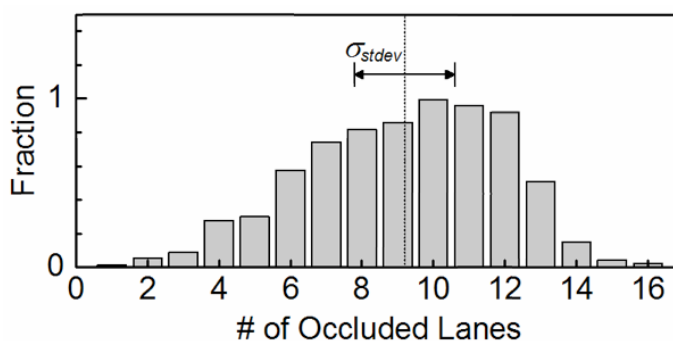


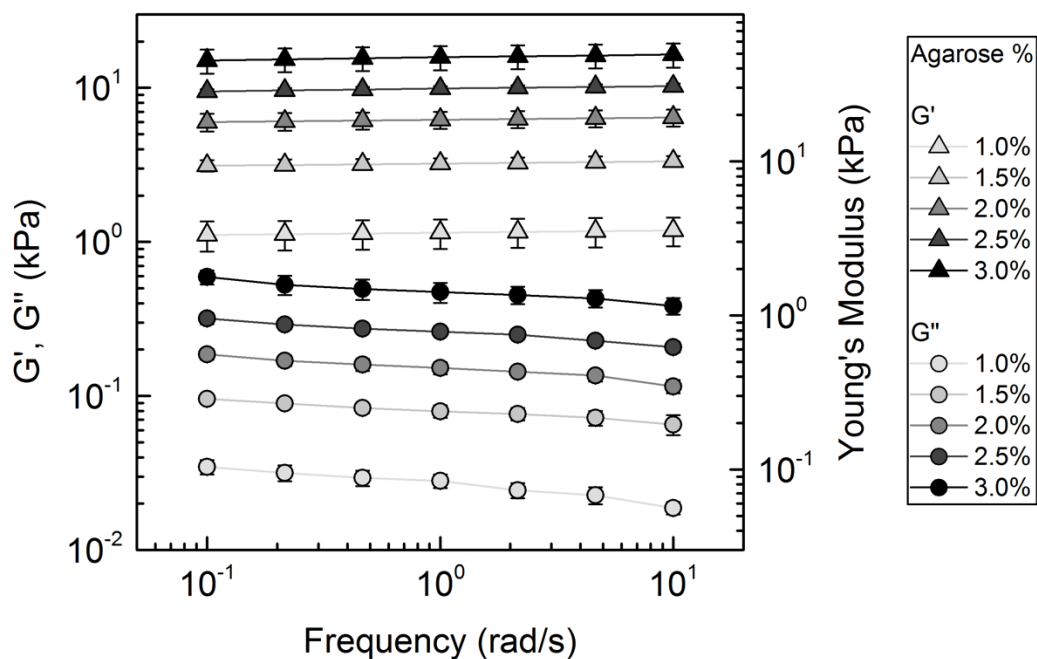
## Supplemental Figures



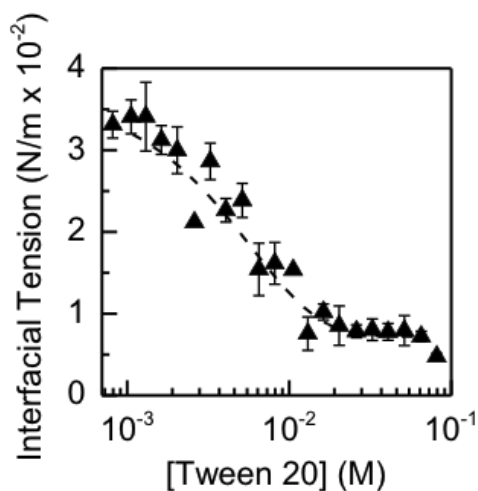
**S. Fig. 1. Effect of Pluronic F-127 on HL-60 cell transit time.** Devices +F-127 pretreatment: microfluidic devices are pretreated with 0.1% (w/w) Pluronic F-127 in RPMI medium for 1 hour prior to flowing cells through the device. +F-127: 0.1% (w/w) Pluronic F-127 is added to the cell suspension as denoted by the red boxplots. Boxplots show medians denoted by the line, interquartile ranges represented by boxes, and 10<sup>th</sup> and 90<sup>th</sup> percentiles shown by whiskers.  $N > 120$  cells for each sample.



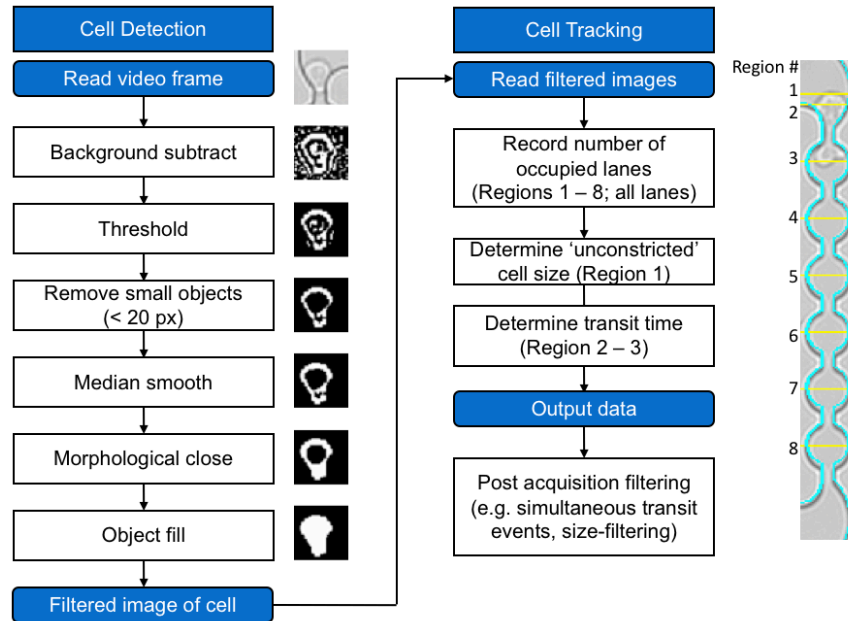
**S. Fig. 2. Simultaneous lane occlusions during transit of WT HL-60 cells.** Histogram of the number of occluded lanes during the transit of each cell. Transit time measurements are performed under standard conditions for HL-60 cells with driving pressure 28 kPa, channel width  $5.3 \times 5.2 \mu\text{m}^2$ . Dotted line represents the mean, while the black arrow represents the standard deviation.



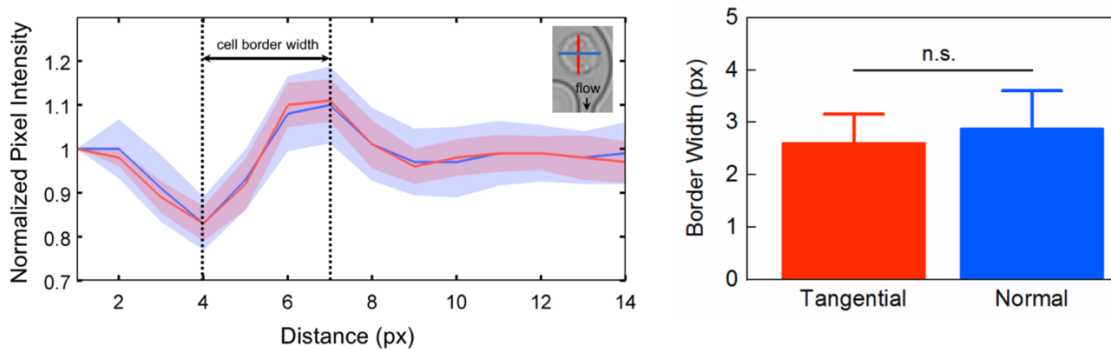
**S. Fig. 3. Mechanical properties of agarose gel slabs.** Rheology measurements of the elastic storage ( $G'$ ) and viscous loss ( $G''$ ) moduli (left axis) of low gel-temperature agarose gels as a function of agarose density (w/w%). To calculate the Young's modulus (right axis, triangles), we use a Poisson ratio of 0.5. Error bars represent  $\pm 1$  standard deviation for  $N = 3$  replicates at each agarose density.



**S. Fig. 4. Interfacial tension as a function of Tween 20 concentration.** Interfacial tension measured by the pendant drop technique. Data points represent the average interfacial tension obtained from independent experiments ( $N = 3$ ). Error bars represent the standard deviation.



**S. Fig. 5. Flowchart illustrating the algorithm used for image analysis.** Images show a representative HL-60 cell flowing through a constriction with a  $5.3 \mu\text{m}$  height  $\times$   $5.2 \mu\text{m}$  width.



**S. Fig. 6. Quantification of object blurring during cell transit.** Image blurring is assessed by measuring the width of the cell border in directions both tangential and normal to flow. Bar plots represent the average border width. Error bars denote the standard deviation ( $N = 35$ ).

## Supplemental Video

**S.Video. 1. Pluronic F-127 can minimize cell-wall adhesion during transit through a PDMS microfluidic device.** Pancreatic ductal epithelial (HPDE) cells transiting through  $9 \times 10$  constrictions (A) without Pluronic F-127, and (B) with 0.1% (w/w) Pluronic F-127 in the cell media. While we qualitatively observe a difference in the transit behavior of these pancreatic ductal epithelial (HPDE) cells, other cell types, such as HL-60 cells, show no significant difference in transit times with and without Pluronic F-127 surfactant (S. Fig. 1). Videos are acquired at 2000 fps. Videos are slowed down by 10x.